ARTICLE
Journal of Cellular Biochemistry 112:3206–3215 (2011)

Journal of Cellular Biochemistry

Deregulated HOX Genes in Ameloblastomas Are Located in Physical Contiguity to Keratin Genes

Giulia Schiavo,[1] Vincenzo D'Antò,[2] Monica Cantile,[3] Alfredo Procino,[4] Stefano Di Giovanni,[4] Rossella Valletta,[2] Luigi Terracciano,[1] Daniel Baumhoer,[1] Gernot Jundt,[1] and Clemente Cillo[4]*

[1] *Institute of Pathology—Molecular Pathology Division, University of Basel, Schonbeinstrasse 40, 4031 Basel, Switzerland*

[2] *Department of Oral and Maxillofacial Sciences, Federico II University, Naples, Italy*

[3] *Surgical Pathology Department, National Cancer Institute "G. Pascale," Naples, Italy*

[4] *Department Clinical & Experimental Medicine Federico II University Medical School Via S. Pansini 5, 80131 Naples, Italy*

ABSTRACT

The expression of the HOX gene network in mid-stage human tooth development mostly concerns the epithelial tooth germ compartment and involves the C and D HOX loci. To further dissect the HOX gene implication with tooth epithelium differentiation we compared the expression of the whole HOX network in human ameloblastomas, as paradigm of epithelial odontogenic tumors, with tooth germs. We identified two ameloblastoma molecular types with respectively low and high number of active HOX C genes. The highly expressing HOX C gene ameloblastomas were characterized by a strong keratinized phenotype. Locus C HOX genes are located on chromosome 12q13–15 in physical contiguity with one of the two keratin gene clusters included in the human genome. The most posterior HOX C gene, HOX C13, is capable to interact with hair keratin genes located on the other keratin gene cluster in physical contiguity with the HOX B locus on chromosome 17q21–22. Inside the HOX C locus, a 2.2 kb ncRNA (HOTAIR) able to repress transcription, *in cis*, along the entire HOX C locus and, *in trans*, at the posterior region of the HOX D locus has recently been identified. Interestingly both loci are deregulated in ameloblastomas. Our finding support an important role of the HOX network in characterizing the epithelial tooth compartment. Furthermore, the physical contiguity between locus C HOX and keratin genes in normal tooth epithelium and their deregulation in the neoplastic counterparts suggest they may act on the same mechanism potentially involved with epithelial tumorigenesis. J. Cell. Biochem. 112: 3206–3215, 2011.

KEY WORDS: HOX GENES; HOX AND AMELOBLASTOMAS; HOX AND KERATINS

Odontogenic tumors of the jawbones are lesions arising from epithelial, ectomesenchymal, and/or mesenchymal tissues representing parts of the tooth-forming apparatus [Philipsen and Reichart, 2006]. Solid/multicystic ameloblastomas are epithelial and locally invasive tumors that represent the second most common tumor type of all odontogenic tumors [Jundt and Reichart, 2008]. They typically grow slowly and often recur after incomplete excision but virtually never metastasize [Gardner, 1996]. Most of the ameloblastomas develop in the posterior region of the mandible and display heterogeneous gene expression patterns compared with human tooth germs [Carinci et al., 2004; Ruhin-Poncet et al., 2009]. Ameloblastomas show two distinct histopathological patterns without clinical importance. Whereas the follicular subtype demonstrates islands of odontogenic epithelium resembling the enamel organ within a fibrous stroma, the plexiform subtype shows anastomosing strands of primarily basal cells with an inconspicuous stellate reticulum [Gardner, 1996]. The expression of different keratins (CK8, CK19, AE1/AE3) has been described in distinct

Potential conflict of interest: Nothing to report.

Reference Register of the German-Austria-Swiss working group of tumours of the jaws (DOESAK).

Grant sponsor: Oncosuisse (Krebsliga Schweiz) KLS; Grant number: 02005-02-2007; Grant sponsor: Krebsliga Beider Basel; Grant number: KLBB 06/2006; Grant sponsor: PRIN (Italy); Grant number: 2006069951_003.

*Correspondence to: Clemente Cillo, Via S. Pansini 5, Naples 80131, Italy. E-mail: clecillo@unina.it

Received 17 May 2011; Accepted 22 June 2011 • DOI 10.1002/jcb.23248 • © 2011 Wiley Periodicals, Inc.
Published online 5 July 2011 in Wiley Online Library (wileyonlinelibrary.com).

histologic variants of ameloblastomas [Wato et al., 2006]. A prominent squamous metaplasia within the stellate reticulum-like areas, for example, that can progress to keratin pearl formation is a well-recognized feature of acanthomatous ameloblastoma [Gardner, 1996].

Although several studies have detected genetic and cytogenic alterations in epithelial odontogenic tumors [Gollin and Janecka, 1994; Kumamoto, 2006], the molecular pathogenesis of benign and malignant odontogenic tumors has not been extensively investigated. The fos oncogene and tumor necrosis factor receptor 1 (TNFRSF1A) are hyper-expressed in ameloblastomas [Heikinheimo et al., 2002]. Sonic hedgehog (SHH), cadherins 12 and 13 and transforming growth-factor beta 1 (TGFβ1) are under-expressed in ameloblastomas with respect to their expression in normal tooth development [Heikinheimo et al., 2002]. The development and progression of odontogenic tumors are affected by alterations of the molecular mechanisms associated with tooth development and bone metabolism involving a cross talk between the SHH and the PI3K signaling with the convergence of these signals to the regulation of Gli transcription factors [Sauk et al., 2010].

Class I Homeobox genes (Hox in mice, HOX in human) are transcription factors mostly involved in embryonic development [Gehring and Hiromi, 1986]. They display an unique genomic network organization: four compact chromosomal loci [HOXA at 7p15.3, HOXB at 17q21.3, HOXC at 12q13.3 and HOXD at 2q31—Apiou et al., 1996] where 39 sequence corresponding genes can be aligned with each other into 13 antero-posterior paralogous groups. The HOX gene network, the most repeat-poor regions in the human genome [Lander et al., 2001], is also expressed in normal adult human organs [Cillo et al., 2001]. Homeobox and HOX genes appear to regulate phenotype cell identity [Cillo et al., 1999], cell differentiation [Magli et al., 1991; Cantile et al., 2003a] and control primary cellular processes, as proven by the description of congenital [Mortlock and Innis, 1997], somatic [Nakamura et al., 1996] and metabolic [Ferber et al., 2000] diseases involving these genes. Besides the already established role in hematopoiesis and leukemogenesis [Argiropoulos and Humphries, 2007], the HOX network is implicated in the neoplastic alterations of human solid tissues and organs such as kidney, colon, lung, skin, bladder, liver, breast, and prostate [Cillo, 1994–95; Abate-Shen, 2002]. New crucial functions have recently been ascribed to HOX genes and homeoproteins mostly related to their interaction with miRNAs and non-coding RNAs to guarantee export and transcription of specific mRNAs [Cobb and Duboule, 2004; Rinn et al., 2007].

The lack of HOX A2 expression in the first branchial arch during embryonic development has suggested the exclusion of HOX genes from the homeobox odontogenic code, postulated to decode the rules of the first branchial arch patterning [Thomas and Sharpe, 1998]. The unsuspected expression of the HOX gene network, which we have reported in human tooth germs between 18 and 24 weeks of development, mostly concerns the epithelial tooth germ compartment. In contrast the HOX network appears to be weakly active in the ectomesenchymal tooth germ compartment as well as in embryonic retro molar tissues [D'Antò et al., 2006].

To further dissect the HOX gene involvement with tooth epithelium differentiation, here we have compared the expression of the HOX network, at mRNA and protein level, in human ameloblastomas, as paradigm of tumors derived from the odontogenic epithelium, with the same expression in human tooth germs.

MATERIALS AND METHODS

TISSUE SAMPLES

Ameloblastoma: Ten frozen ameloblastoma biopsies were collected by searching the files of the Pathology-Institute of the University of Basel, Switzerland. The specimens were obtained from the mandibles of seven males and three females ranging in age from 22 to 60 years (mean age, 34). The cases were included in the Referente Register of the German-Austria-Swiss working group of tumors of the jaws (DOESAK). The histological classification was carried out according to the WHO histological typing criteria for odontogenic tumors and showed three follicular, six plexiform and one desmoplastic ameloblastoma subtypes [Gardner, 1996].

Tooth germ: Human fetal samples were obtained from legally approved therapeutic abortions at the Department of Pathology, University of Naples Federico II. The sampling was carried out according to the University's Guidelines for Human Experimentation (autopsy protocol). Informed consent was obtained from the parents of all the subjects involved in the experiments and the study protocols were reviewed and approved by the University Ethical Committee. The age of the fetuses was calculated from anamnestic and ultrasonographic data, it ranges from 18 to 24 gestational weeks. Tissue samples were collected, typically within 2 h after death. Lower and/or upper jaw were removed. Blocks of the upper and lower jaw were sectioned, including the deciduous tooth germs of incisors and first molar. We also removed blocks of mandibular branch as a control tissue free of tooth germ. Each tissue sample was split into two upright parts, one to be fixed and paraffin embedded, the other to be snap-frozen in liquid nitrogen and stored at −80°C until used for RNA extraction. Sections from the paraffin blocks were stained with hematoxylin and eosin for morphological examination [D'Antò et al., 2006].

IMMUNOHISTOCHEMISTRY

Standard indirect immunoperoxidase procedures were done by immunohistochemistry according to the manufacturer's instructions (VECTASTAIN® Elite ABC Kit, Vector Laboratories, Burlingame, CA). Optimal dilutions were predetermined in our laboratory. Characteristics of all antibodies used are listed in Table I.

RNA EXTRACTION AND ANALYSIS

Total RNA was isolated from frozen biopsies using RNeasy Mini Kit (Qiagen GmbH, Hilden, Germany) following the manufacturer's instructions. Samples were treated with RNase-free DNase (Qiagen GmbH) to prevent amplification of genomic DNA. One microgram RNA was subjected to cDNA synthesis for 1 h at 37°C using the Ready to go You-Primer First-Strand Beads kit (Amersham Biosciences cod. 27-9264-01) in a reaction mixture containing 0,5 μg random hexamers (GeneAmp RNA PCR Random Hexamers Set N808-0127 Applied Biosystems, Foster City, CA).

TABLE I. Characteristics of Antibodies

Antibody	Clone	Dilution	Pretreatment	Chromogen	Manufacturer
HOX C4	ab55245	1:1,000	1	DAB	1
HOX B6	sc-17171	1:100	1	DAB	2
HOX D9	sc-8320	1:100	1	DAB	2
Cytokeratin 22	Mixture	1:500	2	DAB	3

1, microwave pretreatment (120°C, 15 min) in target retrieval solution (DAKO, Glostrup, Denmark); 2, pretreatment (37°C, 38 min) in Ventana Cell Conditioner 1 (Ventana Medical Systems, Inc., Tucson, AZ), DAB, diamino-benzidine.
Manufacturers: 1, Abcam (Cambridge, MA); 2, Santa Cruz Biotechnology, Inc. (Santa Cruz, CA), 3 = Biomeda (Foster City, CA).

PCR AMPLIFICATION

PCR amplification of cDNA was done in a reaction mixture (Pure Taq Ready to go PCR-beads GE Healthcare) containing 4 μl of cDNA sample and different HOX primer sets (20 p/mol each), and human b-actin gene, as an internal control, as previously reported [Cantile et al., 2003b]. To prevent genomic DNA contamination, primer sense and anti-sense were designed to frame a sequence that crossed an intron. The co-amplification of each specific gene and human β-actin gene, as an internal control, was achieved using two primer sets in a single reaction mixture. We selected two pairs of β-actin primers to obtain amplified fragments with different molecular weight (149 and 433 bp), to be used alternatively in the co-amplification reaction. Duplex-PCR products were separated by ethidium 1.2% agarose gel electrophoresis.

REAL-TIME PCR

TaqMan® analysis was carried out on a 7900HT Sequence Detection System. Singleplex PCR reactions were done in Fast Gene Quantification in 96-Well Plates with The TaqMan® Fast Universal PCR Master Mix (10 μl) in a volume of 20 μl containing 2 μl of cDNA and 1 μl of specific TaqMan® Gene Expression Assays for human HOXC (HOXC4, HOXC5, HOXC6, HOXC8, HOXC9, HOXC10, HOXC11, HOXC12, HOXC13) genes and Keratins (KRT1, KRT2, KRT4, KRT5, KRT6, KRT7, KRT8), according to the manufacturer's directions. All reactions were done in triplicate. All reagents were from Applied Biosystems. The comparative Ct method (ref) was employed to determine the human HOXC and Keratins genes variation, using as reference gene TaqMan® Endogenous Controls Human ACTB (b-actin) Endogenous Control (Applied Biosystems).

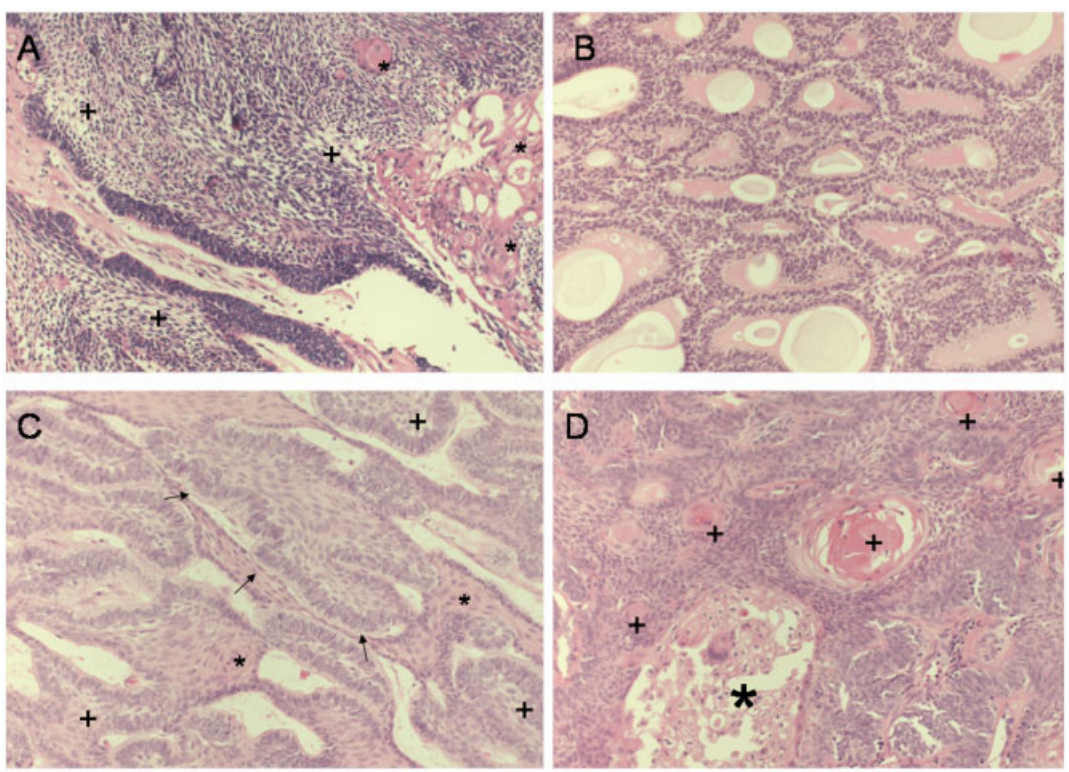

Fig. 1. A: Follicular ameloblastoma with peripheral palisading of tumor cells, reverse polarity of nuclei and focal keratinization (*). Loosening of centrally located cells adding a stellate reticulum like appearance to these areas (+). B: Plexiform ameloblastoma with anastomosing slender strands of tumor cells with peripheral palisading and prominent cystic transformation. C: Plexiform ameloblastoma with pronounced peripheral palisading, reversed polarity and subnuclear vacuoles (arrows). Focal whorl-like arrangement (incipient keratinization*) or stellate-reticulum like disaggregation (+) of central tumor cells. D: Plexiform ameloblastoma with prominent keratinization including horn pearls (+). Some of these areas show an acantholytic change (*). [Color figure can be seen in the online version of this article, available at http://wileyonlinelibrary.com/journal/jcb]

We identified as calibrator a pull of RNAs of the 10 tooth germs that represents the unitary amount of the interested target, consequently the samples express n-fold mRNA relative to the calibrator. Final amounts of target were determined as follows: target amount $= 2^{-Ct}$, where $C_t = [C_t \text{ (HOXC or Keratin genes)} - C_t \text{ (ACTB)}]_{sample} - [C_t \text{ (HOXC or Keratin genes)} - C_t \text{ (ACTB)}]_{calibrator}$.

RESULTS

The 10 ameloblastoma samples of our study were chosen according to the availability of paraffin embedded and fresh frozen tissues of the same tumors. The characteristic morphology of the included ameloblastoma subtypes are shown in Figure 1 as follicular ameloblastomas (Fig. 1A), plexiform ameloblastomas (Fig. 1B) and plexiform ameloblastomas with incipient (Fig. 1C/sample A5 Fig. 2A) and prominent (Fig. 1D/sample A6 Fig. 2A) keratinization.

In Figure 2 the expression of the whole HOX gene network, as detect by duplex RT-PCR, is compared between the ameloblastoma samples (Fig. 2A) and ten tooth germs at 18–24 weeks of embryonic development (Fig. 2B). The HOX network appears, in general, to display an increasing number of active HOX genes in tooth germs *versus* ameloblastoma: the genes HOXA2 and HOXA9 on locus A, HOX B1 on locus B, HOXC8, HOXC10 and HOXC11 on locus C and HOXD12 and HOXD13 on locus D, are more frequently active in tooth germs. In contrast, HOXA1, HOXB13, HOXC4, HOXC5, and HOXC9 increase their frequency of expression in ameloblastomas as compared with tooth germs. Locus HOX C appears to be the HOX locus displaying the most significant changes in the frequency of HOX gene expression both comparing ameloblastoma and tooth germs and between ameloblastoma samples. According to the total number of active HOX genes, 8/10 ameloblastomas of our series display a low number (13-20/39) of active HOX genes in the network (Fig. 2A) whereas the ameloblastoma samples A5 and A6 manifest a high number (26-27/39) of active HOX genes in the network (Fig. 2A).

The histograms reported on Figure 3 compare the HOX genes actively expressed in ameloblastomas and tooth germs according to the HOX network loci and paralogous groups organization as a percentage of active HOX genes over the total number of HOX genes per locus. In Figure 3A, the ameloblastomas with low number of active HOX genes (striped bars) manifest an unaltered ratio of

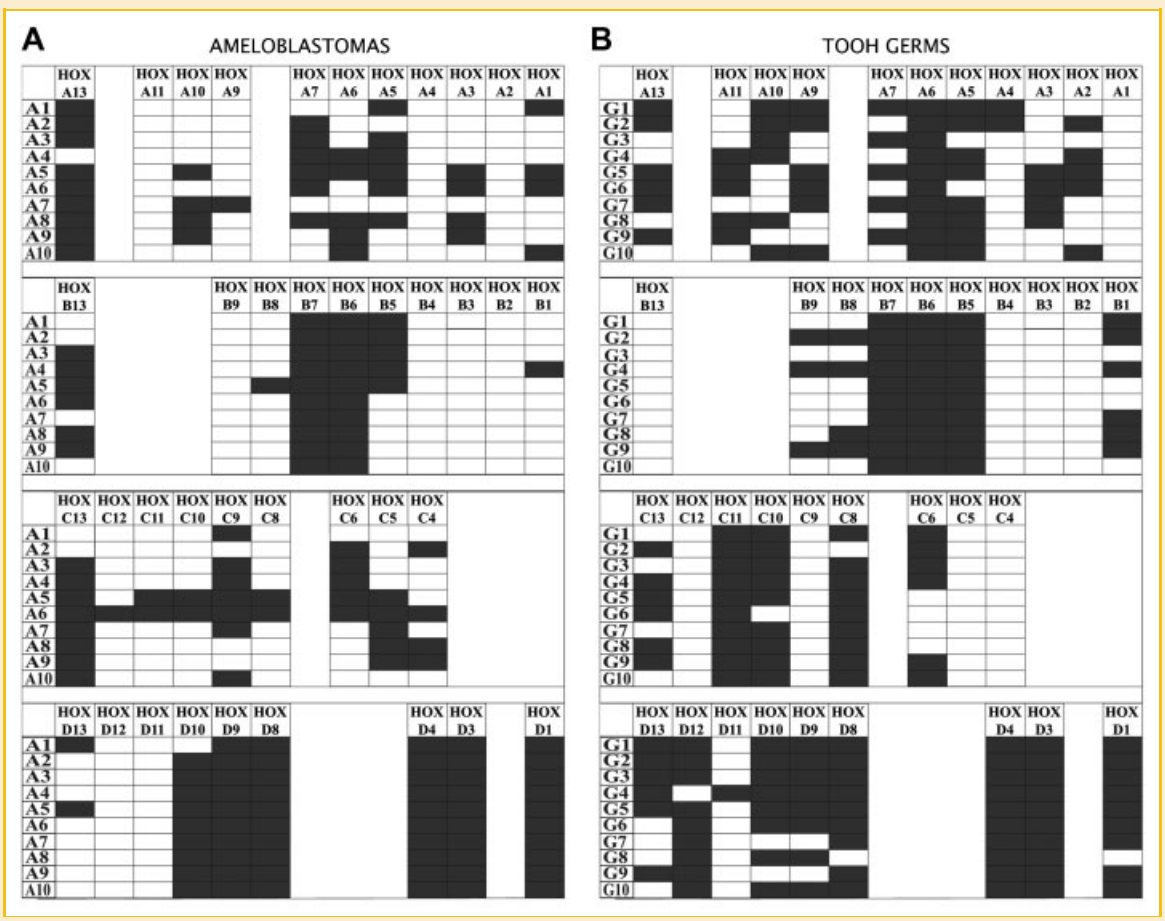

Fig. 2. RT-PCR expression of the HOX gene network in ten ameloblastomas, A1–A10 (A), and 10 tooth germs, G1–G10 (B). The vertical alignment identifies the HOX gene network expression of locus A, B, C, and D genes in ameloblastomas and tooth germs arranged according to paralogous groups 1–13 organization. Black and white small rectangles indicate active or silent HOX genes, respectively.

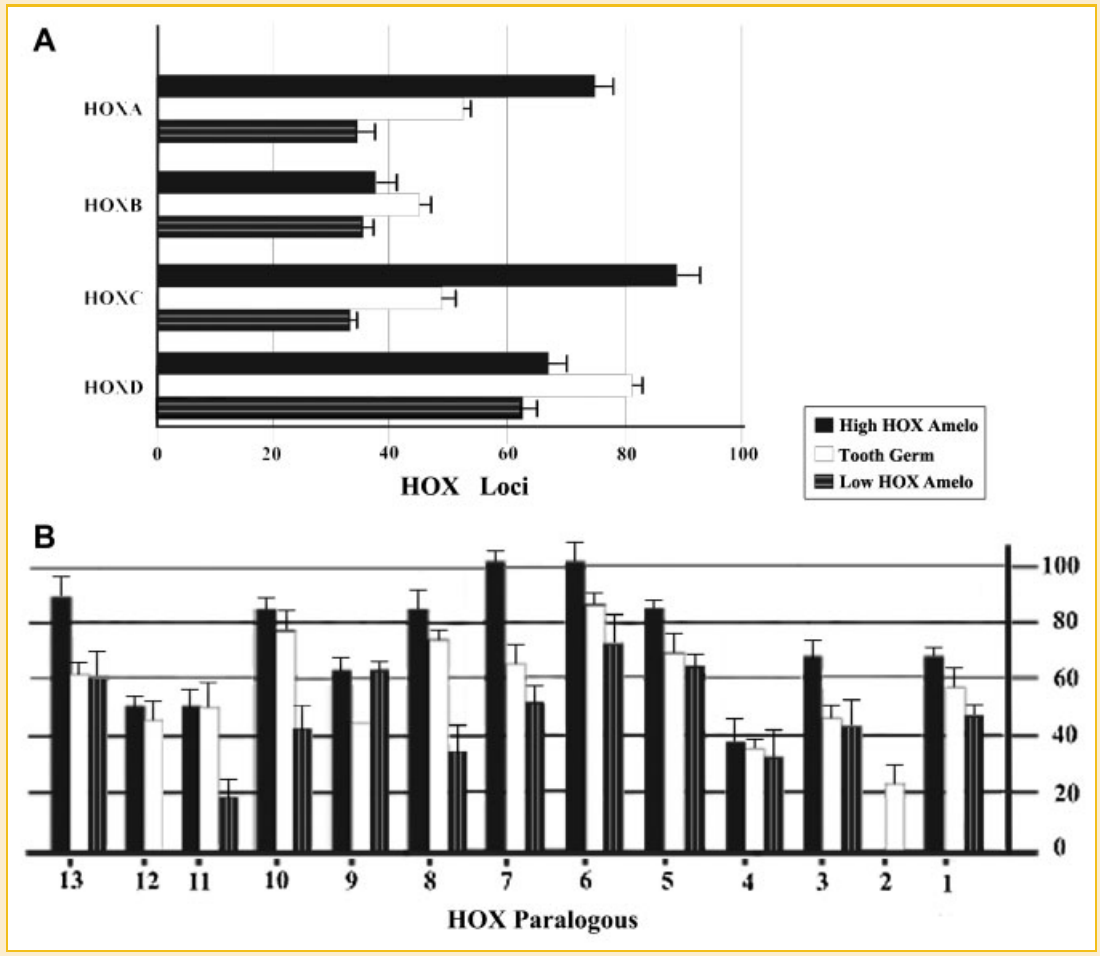

Fig. 3. A: The histogram represents the comparison of the duplex RT-PCR mRNA expression of the HOX gene network between ameloblastomas and tooth germs (white bars) as detected for ameloblastomas displaying low number of active HOX genes (striped bars) and ameloblastomas displaying high number of active HOX genes (black bars). HOX genes are arranged according to the HOX network loci organization HOXA, HOXB, HOXC and HOXD. The X-axis of the histograms represents the percentage of actively expressed HOX genes over the total number of the HOX genes tested. B: The histogram represents the comparison of the duplex RT-PCR mRNA expression of the HOX gene network between ameloblastomas and tooth germs (white columns) as detected for ameloblastomas displaying low number of active HOX genes (striped columns) and ameloblastomas displaying high number of active HOX genes (black columns). HOX genes are arranged according to the HOX network paralogous groups organization from 1 (anterior) to 13 (posterior). The Y-axis of the histograms represents the percentage of actively expressed HOX genes over the total number of the HOX genes tested.

expression between HOX loci as compared with the frequency of the HOX loci expression in tooth germs (white bars) with a decreading expression frequency going from locus HOX D to HOX B, HOX A and HOX C. In contrast, the ratio of expression between HOX loci in the two ameloblastomas with high number of active HOX genes (black bars) is heavily altered with an exceedingly frequency of the HOX C and HOX A loci genes with respect to tooth germs.

In the low expressing ameloblastomas of Figure 3B (striped columns) only 2 paralogous groups HOX genes display a similar (13) or an exceeding (9) frequency of expression versus tooth germs (white columns). In contrast, 12 out of 13 paralogous groups HOX genes display a similar (3 groups) or an increased (9 groups) frequency of expression in the high HOX expressing ameloblastomas (black columns) versus tooth germs, and these paralogous groups manifest a posterior localization inside the HOX network (from groups 5 to 13). Paralogous group 2 HOX genes are undetectable in ameloblastomas. Thus, in spite of the low number of cases, according to the HOX network expression the two group of ameloblastoma appear to fit with different molecular identities.

On the basis of the large differences of locus C HOX gene expression between the two ameloblastoma identities, we have quantified, in real time, locus HOXC gene mRNA expression in ameloblastoma samples versus a pool of the 10 tooth germ RNAs (Fig. 4). Locus C HOX genes display a marked increase of mRNA expression in the samples A5 and A6. Most of the investigated ameloblastoma demonstrated a substantial increase concerning only HOXC4 and HOX C5 mRNAs expression. The most 5′ end HOXC locus gene, HOXC13, already reported to be deregulated in ameloblastomas [Zhong et al., 2007], display a slight increase of mRNA expression in the 6 out of 10 ameloblastoma samples and a peak of mRNA expression in the samples A5 and A6. HOXC6, HOX C9, HOXC10, and HOX C13 revealed a decreased mRNA expression

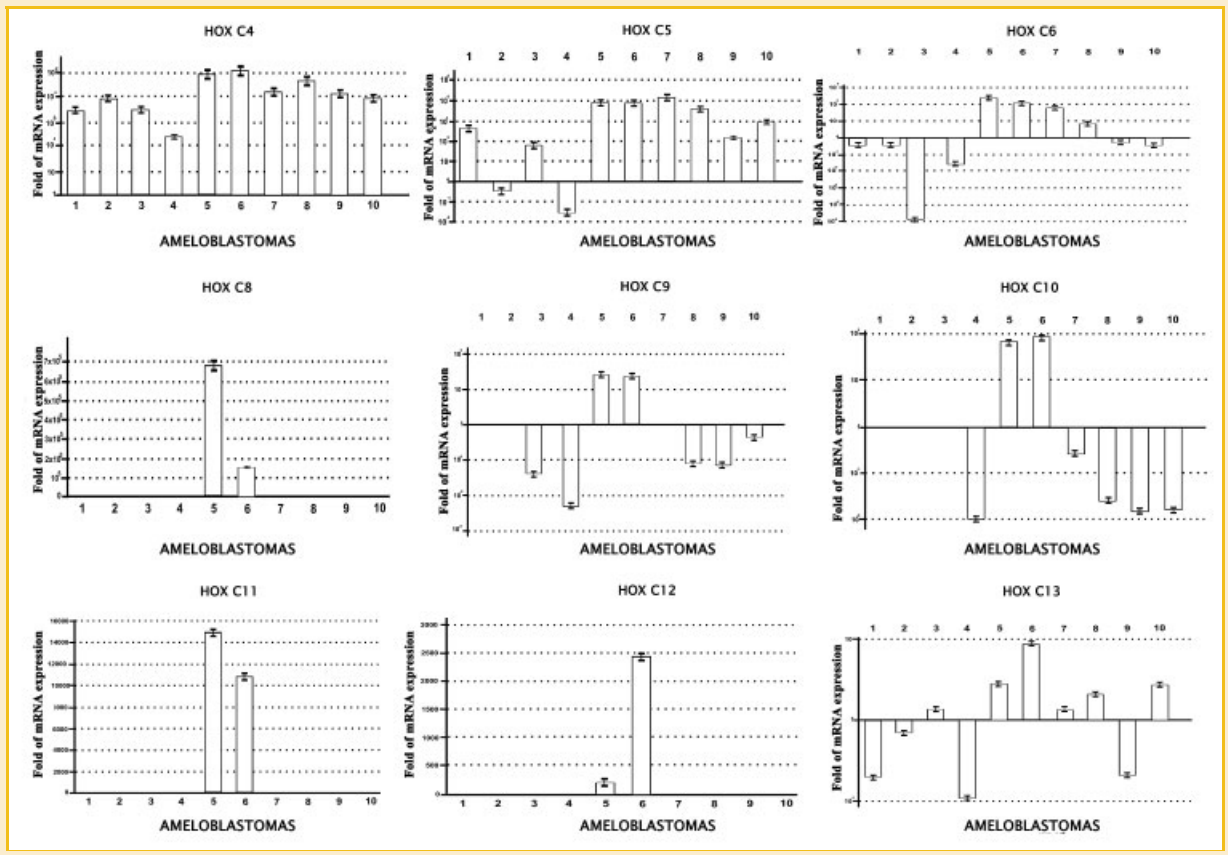

Fig. 4. Real time expression of locus C HOX genes in ameloblastoma samples. Fold increase or decrease in locus C HOX gene expression in 10 ameloblastomas versus a pull of 10 tooth germ RNAs. All reactions were done in triplicate and data are expressed as mean of relative amount of mRNAs levels.

in ameloblastoma samples with respect to tooth germs. Thus, real time quantification validates the initial detection of HOX gene expression by RT-PCR.

The immunoreaction of representative ameloblastoma samples with antibodies against HOXB6, HOXC4, and HOXD9 is shown in Figure 5. Although with a different degree of nuclear/cytoplasmic positivity (more nuclear for HOXB6 and nucleo/cytoplasmic for HOXC4 and HOXD9) the homeoprotein's staining support mRNA expression also in conjunction with the functional characteristics of the markers: HOXD9 is an epithelial determinant, HOXC4 is an immuno/epithelial related transcription factor and HOXB6 deregulation has been connected to autosomal recessive dysmorfic facies

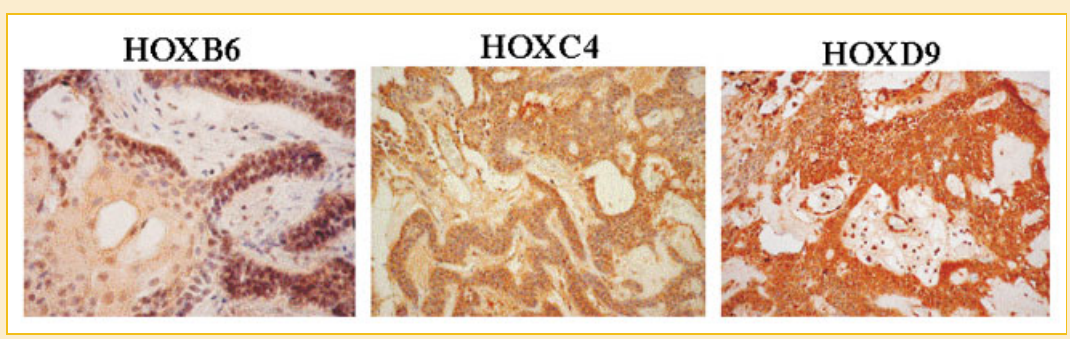

Fig. 5. Immunohistochemical localization of HOXD9, HOXC4, and HOXB6 homeoprotein expression in ameloblastomas. A: HOX B6 immunoreactivity is almost restricted to nuclei especially of peripheral located ameloblastoma cells. Immunoreactivity decreases towards the center of tumor cell nests that exhibit a squamous metaplasia and loosening similar to stellate reticulum. B: Moderate cytoplasmic immunolabeling with anti HOX C4-antibodies. About half of all the nuclei also react with this antibody. Intensity of staining is stronger in nuclei than in the cytoplasm. C: Strong cytoplasmic anti HOX D9-immunoreactivity in all tumor cells. Although some nuclei are completely negative, others present nuclear staining, which, however, is much more pronounced in the nuclei of endothelial cells. [Color figure can be seen in the online version of this article, available at http://wileyonlinelibrary.com/journal/jcb]

syndrome [Al-Owain et al., 2010]. The previously reported localization of the HOXB6 and HOXD9 homeoproteins in human tooth germs, between the 18th and the 24th week of development, mostly concerned the epithelial tooth compartment [D'Antò et al., 2006].

To investigate a potential connection between HOX and cytokeratin expression we detected the real-time mRNA expression of CKs (CK1, CK2, CK4, CK5, CK7, and CK8) in ameloblastoma samples versus a pool of the 10 tooth germ RNAs as reported on Figure 6. CK8 mRNA is actively expressed in both follicular and plexiform ameloblastoma phenotypes as well as in highly expressing HOXC keratinized ameloblastoma samples A5 and A6. CK1, CK2, CK4, CK5, CK6, CK7 mRNAs are only occasionally over-expressed in our ameloblastoma sample series. Of the two highly expressing locus C HOX gene ameloblastomas, the sample A5 display the expression of CK2, CK5, CK6, CK7 whereas the sample A6 display low levels of CK1, CK5, and CK7. At protein level, the staining of the pan-keratin antibody CK22, reported in Figure 7, confirms the keratin expression in the ameloblastomas of our series.

DISCUSSION

The expression of the HOX gene network, inactive at early phase development, detectable in human tooth germs between 18 and 24 weeks of development, mostly concerns the epithelial tooth germ compartment [D'Antò et al., 2006]. Here, detection of the HOX network expression in human ameloblastomas allows identification of two molecular identities with respectively low (13–20) and high (26–27) number of active HOX genes on the network (39 genes). Most of the differences between the two ameloblastoma types concern locus C HOX gene expression. Locus C HOX gene harbors on chromosome 12q13–15 in close proximity to crucial odontogenic cancer genes such as CDk4, MDM2, and Gli. Furthermore the most posterior gene of the HOX C locus, HOX C13 transcriptionally up-regulate hair keratins (CK32, CK35, and CK37) through its binding to distinct core recognition motifs in the keratin proximal promoters [Jave-Suarez et al., 2002]. The ameloblastoma samples displaying an increasing number of active HOX C locus genes (Fig. 1C,D) are, according to pathologist, both plexiform ameloblastomas, with incipient keratinization Fig. 1C) and prominent keratinization including horn pearls (Fig. 1D). The ameloblastoma samples displaying a low number of active HOX C locus genes manifest only occasionally keratinizing spindle shaped squamous cells or focal keratinization. Thus, the ameloblastomas characterized by the high number of active HOX C genes in the network appear to identify a heavily keratinized phenotype. In the genome, the organization of the human keratin genes occur in two gene clusters: one located on chromosome 12q13.13 and the other on chromosome 17q21.2. Both the human keratin gene clusters are in physical contiguity to the

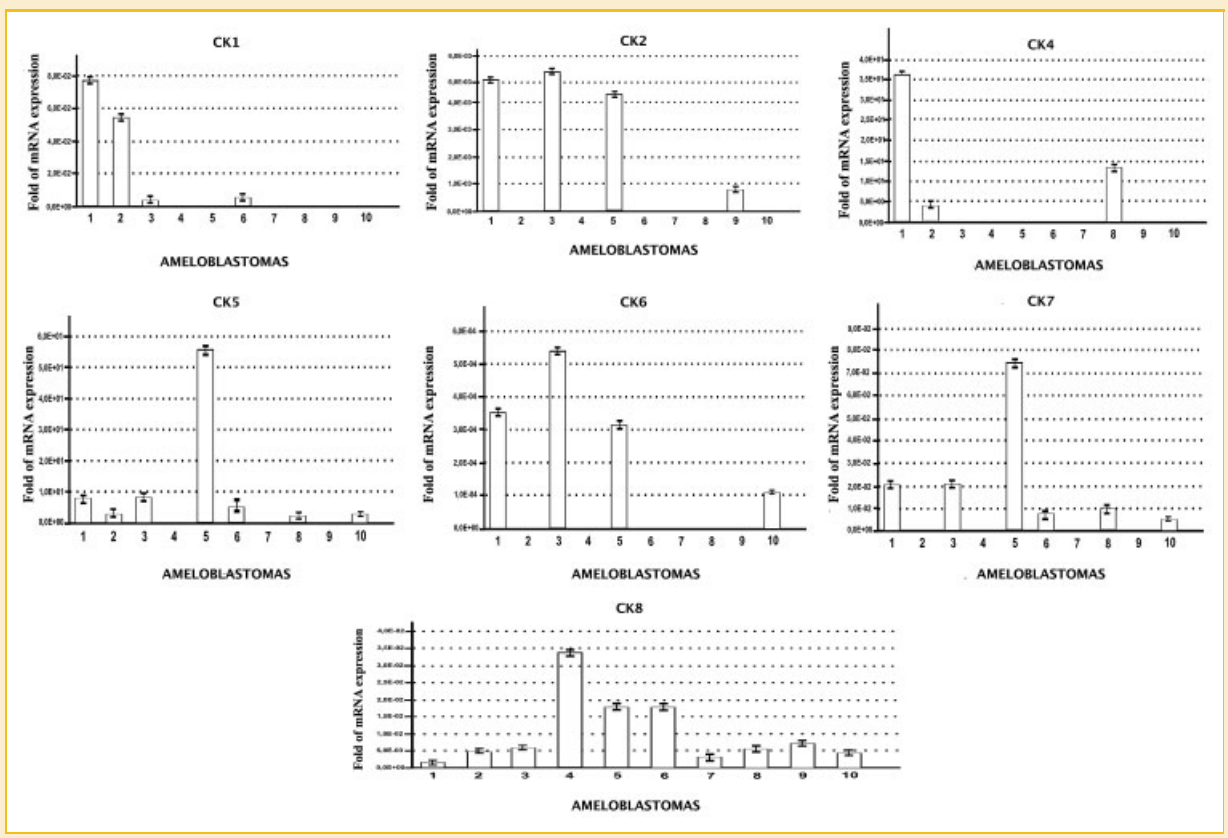

Fig. 6. Real time mRNA expression of keratins in ameloblastoma samples. Fold increase or decrease of keratin gene expression (CK1, CK2, CK4, CK5, CK6, CK7, CK8) in 10 ameloblastomas versus a pull of 10 tooth germ mRNAs. All reactions were done in triplicate and data are expressed as mean of relative amount of mRNAs levels.

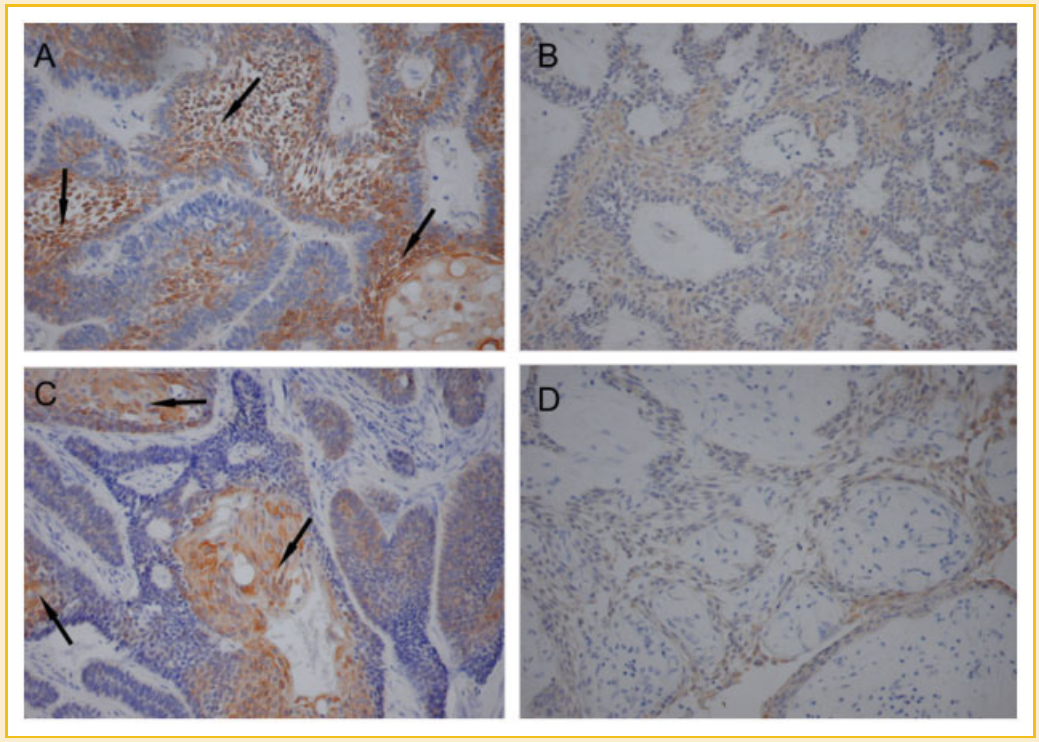

Fig. 7. Immunohistochemical staining of CK22 pan-cytokeratin antibody in follicular (A,C) and plexiform (B,D) ameloblastomas. The staining is mostly restricted, in follicular ameloblastomas to the stellate reticulum-like epithelium (arrows). [Color figure can be seen in the online version of this article, available at http://wileyonlinelibrary.com/journal/jcb]

locus HOX C on chromosome 12 and to the locus HOX B on chromosome 17, respectively. The parallel phylogenetic association of cytokeratin and HOX genes along the human genome evolution has already been demonstrated [Larhammar et al., 2002]. In modern biology the physical contiguity of genes often support an involvement in the same gene program [Misteli, 2004]. On these bases we postulate an interaction between locus C HOX genes and keratins in the regulation of gene expression through the recently reported involvement of keratins in mRNAs transport [Meng et al., 2008] and protein synthesis [Kellner and Coulombe, 2009]. We hypothesize that the interaction between HOX genes and keratins acts as a potential epigenetic resetting of epithelial cells. These mechanisms are functionally integrated in the epithelial tooth compartment and deregulated along the neoplastic evolution of tooth epithelium as occurs in human ameloblastomas.

Although the hyper expressing locus C HOX gene ameloblastomas of our series both display a keratinized phenotype, they do not manifest the same pattern of keratin expression. The sample in Figure 1C exhibits the highest expression of keratins whose genes are located in close proximity of the HOX C locus with respect to any other ameloblastoma. In contrast, Figure 1D sample, that display the complete activation of locus C HOX genes, exhibits the highest HOX C13 expression versus any ameloblastoma of our series. According to the reported role of HOX C13 on the promoter of hair keratins located on chromosome 17 [Jave-Suarez et al., 2002], the keratin expression of Figure 1D sample mostly concerns CK22, a pan-CK cocktail identifying mostly keratins whose genes are localized on chromosome 17.

The coordinate regulation of locus C HOX genes in ameloblastoma suggests the potential presence of a common regulatory mechanism in this chromosomal area. Recently the characterization of the transcriptional landscape relative to the four human HOX loci, at five base pairs resolution, has allowed for identification of a 2.2 kb ncRNA residing in the HOX C locus, termed HOTAIR, which repress transcription, *in cis* along the entire HOX C locus and *in trans* across 40 kb at 5′ end of the HOX D locus [Rinn et al., 2007]. The other part of the HOX network manifesting altered HOX gene expression in our comparison between ameloblastomas and tooth germs is indeed represented by genes located at the 5′ end of the HOX D locus on chromosome 2q31–33. These data are suggestive of the alteration on genes controlling posterior structures [Tschopp and Duboule, 2011], as conformed by the repartition of the HOX gene expression in ameloblastomas according to vertical paralogous groups of Figure 3B in support of the posterior localization of ameloblastomas along the mandibular arch.

In conclusion, the HOX gene deregulation described in ameloblastomas confirms the role played by HOX genes in the characterization of the epithelial tooth compartment. Furthermore the physical contiguity of locus C HOX and keratin genes in the epithelial tooth compartment together with their deregulation occurring along tooth epithelial neoplastic transformation suggest the possibility of a mechanism potentially involved with the epithelial neoplastic transformation of other organs. This observation is supported by the already described deregulation of locus C HOX genes in several types of human carcinomas (bladder, prostate, uterus and kidney) [Cillo et al., 1992; Cantile et al., 2003a; 2005; López et al., 2006].

ACKNOWLEDGMENTS

We thank Prof. G. De Libero for the critical reading of the manuscript and Miss Paula Cullen for the editing.

REFERENCES

Abate-Shen C. 2002. Deregulated homeobox gene expression in cancer: Cause or consequence? Nat Rev Cancer 2:777–785.

Al-Owain M, Alazami A, Alkuraya F. 2010. An autosomal recessive syndrome of severe cognitive impairment, dysmorphic facies and skeletal abnormalities maps to the long arm of chromosome 17. Clin Genet DOI: 10.1111/j.1399-0004.2010.01573.

Apiou F, Flagiello D, Cillo C, Malfoy B, Poupon MF, Dutrillaux B. 1996. Fine mapping of human HOX gene clusters. Cytogenet Cell Genet 73:114–115.

Argiropoulos B, Humphries RK. 2007. Hox genes in hematopoiesis and leukemogenesis. Oncogene 26:568–572.

Cantile M, Cindolo L, Napodano G, Altieri V, Cillo C. 2003a. Hyperexpression of locus C genes in the HOX network is strongly associated in vivo with human bladder transitional cell carcinomas. Oncogene 22:6462–6468.

Cantile M, Procino A, D'Armiento M, Cindolo L, Cillo C. 2003b. HOX gene network is involved in the transcriptional regulation of in vivo human adipogenesis. J Cell Physiol 194:225–236.

Cantile M, Kisslinger A, Cindolo L, Schiavo G, D'Antò V, Franco R, Altieri V, Gallo A, Villacci A, Tramontano D, Cillo C. 2005. cAMP induced modifications of HOX D gene expression in prostate cells allow the identification of a chromosomal area involved in vivo with neuroendocrine differentiation of human advanced prostate cancers. J Cell Physiol 205:202–210.

Carinci F, Palmieri A, Delaiti G, Rubini C, Fioroni M, Martinelli M, Pezzetti F, Scapoli L, Piattelli A. 2004. Expression profiling of ameloblastic carcinoma. J Craniofac Surg 15:264–269.

Cillo C. 1994–1995. HOX genes in human cancers. Invasion Metastasis 14: 38–49.

Cillo C, Barba P, Freschi G, Bucciarelli G, Magli MC, Boncinelli E. 1992. HOX gene expression innormal and neoplastic human kidney. Int J Cancer 5:892–897.

Cillo C, Faiella A, Cantile M, Boncinelli E. 1999. Homeobox genes and cancer. Exp Cell Res 248:1–9.

Cillo C, Cantile M, Faiella A, Boncinelli E. 2001. Homeobox genes in normal and malignant cells. J Cell Physiol 188:161–169.

Cobb J, Duboule D. 2004. Tracing microRNA patterns in mice. Nat Genet 36:1033–1034.

D'Antò V, Cantile M, D'Armiento M, Schiavo G, Spagnuolo G, Terracciano L, Vecchione R, Cillo C. 2006. The HOX genes are expressed, in vivo, in human tooth germs: In vitro cAMP exposure of dental pulp cells results in parallel HOX network activation and neuronal differentiation. J Cell Biochem 97:836–848.

Ferber S, Halkin A, Cohen H, Ber I, Einav Y, Goldberg I, Barshack I, Seijffers R, Kopolovic J, Kaiser N, Karasik A. 2000. Pancreatic and duodenal homeobox gene 1 induces expression of insulin genes in liver and ameliorates streptozotocin-induced hyperglycemia. Nat Med 6:568–572.

Gardner DG. 1996. Some current concepts on the pathology of ameloblastomas. Oral Surg Oral Med Oral Pathol Oral Radiol Endod 82:660–669.

Gehring WJ, Hiromi Y. 1986. Homeotic genes and the homeobox. Annu Rev Genet 20:147–173.

Gollin SM, Janecka IP. 1994. Cytogenetics of cranial base tumors. J Neurooncol 20:241–254.

Heikinheimo K, Jee KJ, Niini T, Aalto Y, Happonen RP, Leivo I, Knuutila S. 2002. Gene expression profiling of ameloblastoma and human tooth germ by means of a cDNA microarray. J Dent Res 81:525–530.

Jave-Suarez LF, Winter H, Langbein L, Rogers MA, Schweizer J. 2002. HOXC13 is involved in the regulation of human hair keratin gene expression. J Biol Chem 277:3718–3726.

Jundt G, Reichart PA. 2008. Benign odontogenic ectomesenchymal tumors. Pathologe 29:199–204.

Kellner JC, Coulombe PA. 2009. Keratins and protein synthesis: The plot thickens. J Cell Biol 187:157–159.

Kumamoto H. 2006. Molecular pathology of odontogenic tumors. J Oral Pathol Med 35:65–74.

Lander ES, Linton LM, Birren B, Nusbaum C, Zody MC, Baldwin J, Devon K, Dewar K, Doyle M, FitzHugh W, Funke R, Gade D, Harris K, Heaford A, Howland J, Kann L, Lehoczky J, LeVine R, McEwan P, McKernan K, Meldrim J, Mesirov JP, Miranda C, Morris W, Naylor J, Raymond C, Rosetti M, Santos R, Sheridan A, Sougnez C, Stange-Thomann N, Stojanovic N, Subramanian A, Wyman D, Rogers J, Sulston J, Ainscough R, Beck S, Bentley D, Burton J, Clee C, Carter N, Coulson A, Deadman R, Deloukas P, Dunham A, Dunham I, Durbin R, French L, Grafham D, Gregory S, Hubbard T, Humphray S, Hunt A, Jones M, Lloyd C, McMurray A, Matthews L, Mercer S, Milne S, Mullikin JC, Mungall A, Plumb R, Ross M, Shownkeen R, Sims S, Waterston RH, Wilson RK, Hillier LW, McPherson JD, Marra MA, Mardis ER, Fulton LA, Chinwalla AT, Pepin KH, Gish WR, Chissoe SL, Wendl MC, Delehaunty KD, Miner TL, Delehaunty A, Kramer JB, Cook LL, Fulton RS, Johnson DL, Minx PJ, Clifton SW, Hawkins T, Branscomb E, Predki P, Richardson P, Wenning S, Slezak T, Doggett N, Cheng JF, Olsen A, Lucas S, Elkin C, Uberbacher E, Frazier M, Gibbs RA, Muzny DM, Scherer SE, Bouck JB, Sodergren EJ, Worley KC, Rives CM, Gorrell JH, Metzker ML, Naylor SL, Kucherlapati RS, Nelson DL, Weinstock GM, Sakaki Y, Fujiyama A, Hattori M, Yada T, Toyoda A, Itoh T, Kawagoe C, Watanabe H, Totoki Y, Taylor T, Weissenbach J, Heilig R, Saurin W, Artiguenave F, Brottier P, Bruls T, Pelletier E, Robert C, Wincker P, Smith DR, Doucette-Stamm L, Rubenfield M, Weinstock K, Lee HM, Dubois J, Rosenthal A, Platzer M, Nyakatura G, Taudien S, Rump A, Yang H, Yu J, Wang J, Huang G, Gu J, Hood L, Rowen L, Madan A, Qin S, Davis RW, Federspiel NA, Abola AP, Proctor MJ, Myers RM, Schmutz J, Dickson M, Grimwood J, Cox DR, Olson MV, Kaul R, Raymond C, Shimizu N, Kawasaki K, Minoshima S, Evans GA, Athanasiou M, Schultz R, Roe BA, Chen F, Pan H, Ramser J, Lehrach H, Reinhardt R, McCombie WR, de la Bastide M, Dedhia N, Blöcker H, Hornischer K, Nordsiek G, Agarwala R, Aravind L, Bailey JA, Bateman A, Batzoglou S, Birney E, Bork P, Brown DG, Burge CB, Cerutti L, Chen HC, Church D, Clamp M, Copley RR, Doerks T, Eddy SR, Eichler EE, Furey TS, Galagan J, Gilbert JG, Harmon C, Hayashizaki Y, Haussler D, Hermjakob H, Hokamp K, Jang W, Johnson LS, Jones TA, Kasif S, Kaspryzk A, Kennedy S, Kent WJ, Kitts P, Koonin EV, Korf I, Kulp D, Lancet D, Lowe TM, McLysaght A, Mikkelsen T, Moran JV, Mulder N, Pollara VJ, Ponting CP, Schuler G, Schultz J, Slater G, Smit AF, Stupka E, Szustakowski J, Thierry-Mieg D, Thierry-Mieg J, Wagner L, Wallis J, Wheeler R, Williams A, Wolf YI, Wolfe KH, Yang SP, Yeh RF, Collins F, Guyer MS, Peterson J, Felsenfeld A, Wetterstrand KA, Patrinos A, Morgan MJ, de Jong P, Catanese JJ, Osoegawa K, Shizuya H, Choi S, Chen YJ, International Human Genome Sequencing Consortium. 2001. Initial sequencing and analysis of the human genome. Nature 409:860–921.

Larhammar D, Lundin LG, Hallböök F. 2002. The human Hox-bearing chromosome regions did arise by block or chromosome (or even genome) duplications. Genome Res 12:1910–1920.

López R, Garrido E, Vázquez G, Piña P, Pérez C, Alvarado I, Salcedo M. 2006. A subgroup of HOX Abd-B gene is differentially expressed in cervical cancer. Int J Gynecol Cancer 16:1289–1296.

Magli MC, Barba P, Celetti A, De Vita G, Cillo C, Boncinelli E. 1991. Coordinate regulation of HOX genes in human hematopoietic cells. Proc Natl Acad Sci USA 88:6348–6352.

Meng LH, Meng Z, Miao ZH, Veenstra TD, Pommier Y. 2008. Cytokeratin-RNA cross-linking mediated by the antitumor aminoflavone, 5-amino-2,3-fluorophenyl-6,8-difluoro-7-methyl-4H-1-benzopyran-4-one. J Pharmacol Exp Ther 325:674–680.

Misteli T. 2004. Spatial positioning; a new dimension in genome function. Cell 119:153–156.

Mortlock DP, Innis JW. 1997. Mutation of HOXA13 in hand-foot-genital syndrome. Nat Genet 15:179–180.

Nakamura T, Largaespada DA, Lee MP, Johnson LA, Ohyashiki K, Toyama K, Chen SJ, Willman CL, Chen IM, Feinberg AP, Jenkins NA, Copeland NG, Shaughnessy JD Jr. 1996. Fusion of the nucleoporin gene NUP98 to HOXA9 by the chromosome translocation t(7;11)(p15;p15) in human myeloid leukaemia. Nat Genet 12:154–158.

Philipsen HP, Reichart PA, Classification of odontogenic tumours. 2006. A historical review. J Oral Pathol Med 35:525–529.

Rinn JL, Kertesz M, Wang JK, Squazzo SL, Xu X, Brugmann SA, Goodnough LH, Helms JA, Farnham PJ, Segal E, Chang HY. 2007. Functional demarcation of active and silent chromatin domains in human HOX loci by noncoding RNAs. Cell 129:1311–1323.

Ruhin-Poncet B, Ghoul-Mazgar S, Hotton D, Capron F, Jaafoura MH, Goubin G, Berdal A. 2009. Msx and dlx homeogene expression in epithelial odontogenic tumors. J Histochem Cytochem 57:69–78.

Sauk JJ, Nikitakis NG, Scheper MA. 2010. Are we on the brink of nonsurgical treatment for ameloblastoma? Oral Surg Oral Med Oral Pathol Oral Radiol Endod 110:68–78.

Thomas BL, Sharpe PT. 1998. Patterning of the murine dentition by homeobox genes. Eur J Oral Sci 106(Suppl 1):48–54.

Tschopp P, Duboule D. 2011. A regulatory 'landscape effect' over the HoxD cluster. Dev Biol 351:288–296.

Wato M, Chen Y, Fang YR, He ZX, Wu LY, Bamba Y, Hida T, Hayashi H, Ueda M, Tanaka A. 2006. Immunohistochemical Expression of Various Cytokeratins in Ameloblastomas. Oral Med Pathol 11:67–74.

Zhong M, Wang J, Gong YB, Li JC, Zhang B, Hou L. 2007. Expression of HOXC13 in ameloblastoma. Zhonghua Kou Qiang Yi Xue Za Zhi 42:43–46.